SUPPORTING INFORMATION

Discovery of an Atropisomeric PI3Kβ Selective Inhibitor Through Optimization of the Hinge Binding Motif

Stephane Perreault,*[,1] Fatima Arjmand,[2] Jayaraman Chandrasekhar,[1] Jia Hao,[1] Kathleen S. Keegan,[1] David Koditek,[2] Eve-Irene Lepist,[†] Clinton K. Matson,[1] Mary E. McGrath,[2] Leena Patel,[1] Kassandra Sedillo,[†] Joseph Therrien,[1] Nicholas A. Till,[†] Adrian Tomkinson,[2] Jennifer Treiberg,[1] Yelena Zherebina,[2] and Gary Phillips.[1]

[1]Gilead Sciences, Inc., 199 E Blaine Street, Seattle, Washington 98102, United States

[2]Gilead Sciences, Inc., 333 Lakeside Drive, Foster City, California 94404, United States

1. QUINOLINE AND BENZIMIDAZOLE SAR

Table S1. Quinoline SAR.

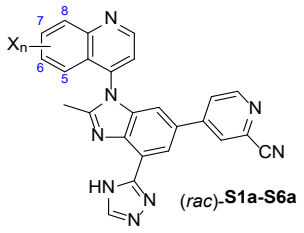

(*rac*)-**S1a-S6a**

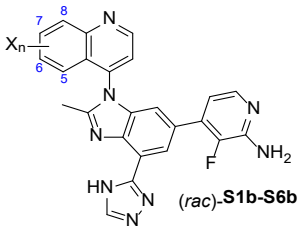

(*rac*)-**S1b-S6b**

X_n	Compound	IC_{50} (nM)[a,b]			Compound	IC_{50} (nM)[a,b]		
		PI3Kβ	PI3Kα	PI3Kδ		PI3Kβ	PI3Kα	PI3Kδ
5,8-difluoro	(*rac*)-**14**	4	48 (120x)	220 (55x)	(*rac*)-**19**	3	260 (87x)	43 (14x)
5,7-difluoro	(*rac*)-**S1a**	5.9	7940 (134x)	120 (21x)	(*rac*)-**S1b**	7.0	550 (79x)	68 (10x)
5-fluoro	(*rac*)-**S2a**	4.6	400 (87x)	120 (26x)	(*rac*)-**S2b**	4.7	220 (48x)	47 (10x)
5-chloro	(*rac*)-**S3a**	198	1200 (6x)	1100 (5x)	--	--	--	--
8-chloro-5-fluoro	(*rac*)-**S4a**	7.0	75 (11x)	20 (3x)	(*rac*)-**S4b**	3.0	30 (10x)	5.0 (<2x)
5-chloro-8-fluoro	(*rac*)-**S5a**	18	1450 (81x)	560 (30x)	(*rac*)-**S5b**	29	1600 (53x)	500 (17x)
5,8-dichloro	(*rac*)-**S6a**	2.8	280 (99x)	78 (28x)	(*rac*)-**S6b**	6.4	430 (68x)	93 (15x)

[a] The activity against each class I PI3K was evaluated in in vitro kinase assays containing 2xK_m steady state concentrations of ATP (average of ≥ 2 determinations). [b] Numbers in parentheses represent fold selectivity (PI3Kα/δ/γ IC_{50} divided by PI3Kβ IC_{50}).

Table S2. Benzimidazole SAR.

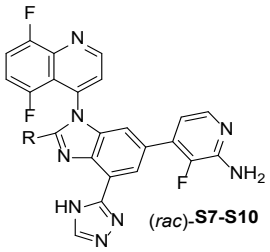

(*rac*)-**S7-S10**

R	Compound	IC_{50} (nM)[a]		
		PI3Kβ	PI3Kα	PI3Kδ
CH_2CH_3	(*rac*)-**S7**	5	320 (64x)	110 (22x)
$(CH_2)_2CH_3$	(*rac*)-**S8**	5	430 (86x)	70 (14x)
	(*rac*)-**S9**	15	1100 (73x)	200 (13x)
	(*rac*)-**S10**	7	420 (60x)	130 (26x)

[a] See footnotes of Table S1.

2. REPRESENTATIVE SYNTHESIS ((*P*)-14)

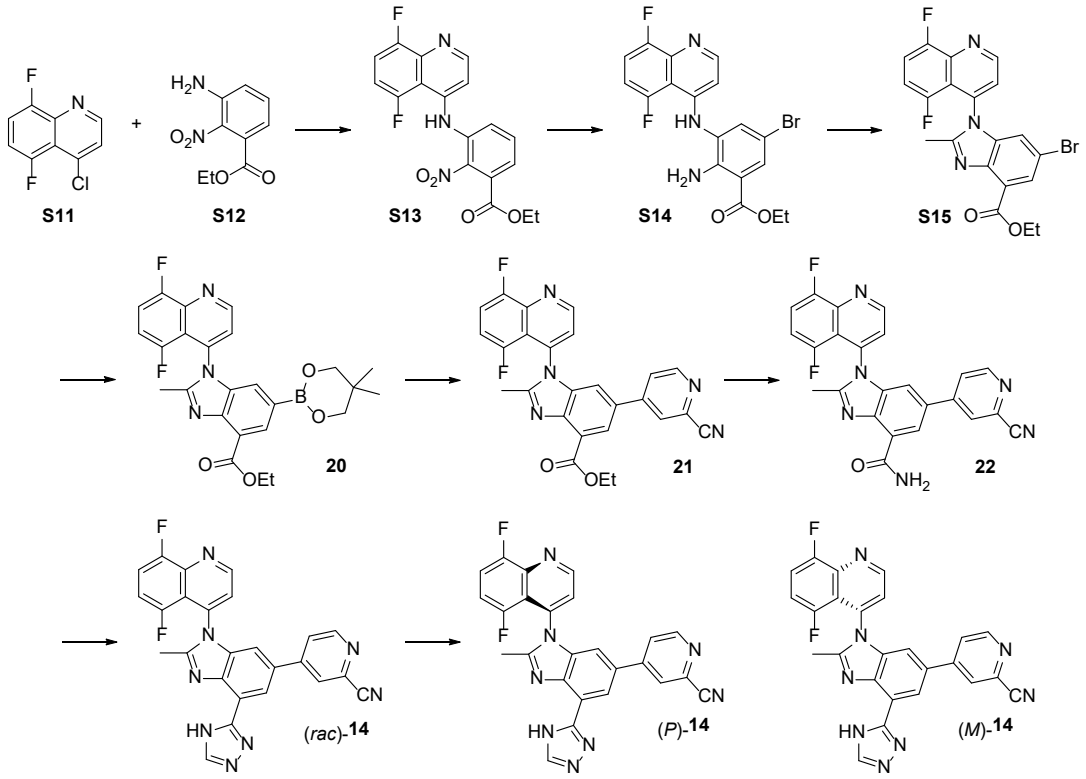

General Procedures. All commercial reagents and anhydrous solvents were used as provided without further purification. Flash chromatography was performed using an ISCO Combiflash or a Biotage Isolera purification system with Silicycle pre-packed silica gel cartridges. Final compounds were purified by prep HPLC on a Gilson 271 system, with a Phenomenex Kinetex C18 Column (250 mm x 30 mm, 100 A, 5 μ) and a gradient elution of acetonitrile/water with, 5-95% for 20 mins at a flow rate of 35 mL/min. For all samples, 0.1% TFA was added to both eluents. All ^{1}H NMR spectra were recorded on a Varian 400-MR 400 MHz spectrometer. Proton chemical shifts are reported in parts per million from an internal standard or residual solvent. The purity of the tested compounds was assessed by an Agilent LCMS. A Silicycle Siliachrom SB C18 column (4.6 x 50 mm, 3 μ) was used with a gradient elution of acetonitrile in water, 0−95% for 7 min at a flow rate of 0.9 mL/min with detection at 256 nm. Alternatively, a Chromolith column (50 x 2 mm) was used with a gradient elution of acetonitrile in water, 0−95% for 3 min at a flow rate of 1.9 mL/min with detection at 256 nm wavelength. For all samples 0.1% TFA was added to both eluents. All final compounds were determined to be at least 95% pure by LC analysis.

Ethyl 3-((5,8-difluoroquinolin-4-yl)amino)-2-nitrobenzoate (S13). To a solution of 4-chloro-5,8-difluoroquinoline (**S11**) (171 g, 859.3 mmol) in DMF (1.7 L) at 0 ºC were added ethyl 3-amino-2-nitrobenzoate (**S12**) (181.5 g, 859.3 mmol) and Cs_2CO_3 (614.4 g, 1890 mmol). The reaction mixture was

stirred at 90 ºC for 18 h. The reaction mixture was cooled down and filtered through a pad of Celite. The filtrate was partitioned between ethyl acetate and water. The organic phase was washed with brine, dried (Na_2SO_4), filtered, and concentrated under reduced pressure. The crude product was purified by silica gel column chromatography, eluting with 30% ethyl acetate in petroleum ether to afford ethyl 3-((5,8-difluoroquinolin-4-yl)amino)-2-nitrobenzoate (**S13**) (158 g, 49%). *m/z* calcd for $C_{18}H_{14}F_2N_3O_4$ $[M+H]^+$ 374.1, found ESI MS *m/z* 374.4 $[M+H]^+$.

Ethyl 2-amino-5-bromo-3-((5,8-difluoroquinolin-4-yl)amino)benzoate (S14). To a solution of **S13** (158 g, 423.5 mmol) in AcOH (1.3 L) and MeOH (320 mL) at 0 ºC was slowly added Zn dust (166 g, 2541 mmol) and the mixture was stirred at ambient temperature for 1 h. The reaction mixture was filtered through a pad of Celite and evaporated under reduced pressure. The resulting residue was suspended in DCM and washed sequentially with an aqueous saturated solution of $NaHCO_3$ and brine. The organic layer was dried (Na_2SO_4), filtered, and concentrated under reduced pressure to give ethyl 2-amino-3-((5,8-difluoroquinolin-4-yl)amino)benzoate (135 g, 93%). *m/z* calcd for $C_{18}H_{16}F_2N_3O_2$ $[M+H]^+$ 344.1, found ESI MS *m/z* 344.0 $[M+H]^+$.

To a solution of ethyl 2-amino-3-((5,8-difluoroquinolin-4-yl)amino)benzoate (135 g, 393 mmol) in DCM (2.7 L) at 0 ºC was added bromine (30.4 mL, 1180 mmol) and the mixture was stirred at 0 ºC for 1 h. The reaction mixture was quenched with aqueous $Na_2S_2O_3$, diluted with DCM and washed sequentially with an aqueous saturated solution of $NaHCO_3$ and brine. The organic layer was dried (Na_2SO_4), filtered, and concentrated under reduced pressure to give ethyl 2-amino-5-bromo-3-((5,8-difluoroquinolin-4-yl)amino)benzoate **(S14)** (103 g, 62%). *m/z* calcd for $C_{18}H_{15}BrF_2N_3O_2$ $[M+H]^+$ 422.0, found ESI MS *m/z* 422.0 $[M+H]^+$.

Ethyl 6-bromo-1-(5,8-difluoroquinolin-4-yl)-2-methyl-1*H*-benzo[*d*]imidazole-4-carboxylate (S15). A solution of **S15** (103 g, 244 mmol) in Ac_2O (515 mL) and AcOH (1 L) was refluxed for 18 h. The reaction mixture was concentrated under reduced pressure. The residue was diluted with ethyl acetate and washed sequentially with an aqueous saturated solution of $NaHCO_3$ and brine. The organic layer was dried (Na_2SO_4), filtered, and concentrated under reduced pressure. The crude compound was triturated with petroleum ether to give ethyl 6-bromo-1-(5,8-difluoroquinolin-4-yl)-2-methyl-1*H*-benzo[*d*]imidazole-4-carboxylate (**S15**) (68 g, 62%). *m/z* calcd for $C_{20}H_{15}BrF_2N_3O_2$ $[M+H]^+$ 446.0, found ESI MS *m/z* 446.2 $[M+H]^+$.

Ethyl 1-(5,8-difluoroquinolin-4-yl)-6-(5,5-dimethyl-1,3,2-dioxaborinan-2-yl)-2-methyl-1*H*-benzo[*d*]imidazole-4-carboxylate (20). [1,1′-Bis(diphenylphosphino)ferrocene]dichloropalladium(II) complex with dichloromethane (1.83 g, 2.24 mmol) was added to a solution of **S15** (10 g, 22.4 mmol),

bis(neopentyl glycolato)diboron (7.6 g, 33.6 mmol) and potassium acetate (5.5 g, 56.0 mmol) in dioxane (150 mL). Nitrogen was bubbled through the reaction mixture for 10 minutes and the reaction mixture was stirred at reflux for 24 h. The reaction mixture was cooled to ambient temperature and the solids were removed by filtration. The filtrate was dry-loaded onto silica gel and purified by silica gel column chromatography eluting with 25 to 100% ethyl acetate in hexane to afford ethyl 1-(5,8-difluoroquinolin-4-yl)-6-(5,5-dimethyl-1,3,2-dioxaborinan-2-yl)-2-methyl-1*H*-benzo[*d*]imidazole-4-carboxylate (**20**) (9.8 g, 91%). *m/z* calcd for $C_{20}H_{16}BF_2N_3O_4$ $[M+H]^+$ 412.1, found ESI MS *m/z* 412.3 $[M+H]^+$ $(ArB(OH)_2+H)^+$.

Ethyl 6-(2-cyanopyridin-4-yl)-1-(5,8-difluoroquinolin-4-yl)-2-methyl-1H-benzo[d]imidazole-4-carboxylate (21). Tetrakis(triphenylphosphine)palladium(0) (1.21 g, 1.04 mmol) was added to a solution of **20** (5.0 g, 10.4 mmol), 2-cyano-4-bromopyridine (2.29 g, 12.5 mmol), and potassium phosphate tribasic (5.54 g, 26.1 mmol) in dioxane (50 mL) and water (12 mL). Nitrogen was bubbled through the reaction mixture for 10 minutes and the reaction mixture was stirred at 70 °C for o/n. Upon cooling to ambient temperature, the reaction mixture was partitioned between ethyl acetate and water. The organic phase was washed with brine, dried with magnesium sulfate, filtered, and concentrated under reduced pressure to about 50 mL. The resulting suspension was stirred 2 h at room temperature and 1 h at 0 °C. The solid was filtered to afford ethyl 6-(2-cyanopyridin-4-yl)-1-(5,8-difluoroquinolin-4-yl)-2-methyl-1H-benzo[d]imidazole-4-carboxylate **(21)** (3.92 g, 80%). *m/z* calcd for $C_{26}H_{18}F_2N_5O_2$ $[M+H]^+$ 470.1, found ESI MS *m/z* 470.1 $[M+H]^+$.

6-(2-cyanopyridin-4-yl)-1-(5,8-difluoroquinolin-4-yl)-2-methyl-1H-benzo[d]imidazole-4-carboxamide (22). Aqueous 1 M lithium hydroxide (25.6 mL) was added to **21** (8.03 g, 17.1 mmol) in THF (85 mL). The reaction was stirred at ambient temperature for 4 h. The reaction mixture was concentrated under reduced pressure to afford lithium 6-(2-cyanopyridin-4-yl)-1-(5,8-difluoroquinolin-4-yl)-2-methyl-1H-benzo[d]imidazole-4-carboxylate, which was used without further purification for the next step. *m/z* calcd for $C_{24}H_{14}F_2N_5O_2$ $[M+H]^+$ 442.1, found ESI MS *m/z* 442.1 $[M+H]^+$.

To a solution of lithium 6-(2-cyanopyridin-4-yl)-1-(5,8-difluoroquinolin-4-yl)-2-methyl-1H-benzo[d]imidazole-4-carboxylate (17.1 mmol) in DMF (80 mL) were added ammonium chloride (5.49 g, 103 mmol), 1*H*-benzo[*d*][1,2,3]triazol-1-ol (7.07 g, 51.3 mmol), *N*1-((ethylimino)methylene)-*N*3,*N*3-dimethylpropane-1,3-diamine hydrochloride (9.83 g, 51.3 mmol) and diethylisopropylamine (24 mL, 137 mmol). The mixture was stirred at 45 °C for overnight. The material was precipitated by the addition of water. The resulting solid was isolated via filtration, washed with water, and dried under vacuum to afford 6-(2-cyanopyridin-4-yl)-1-(5,8-difluoroquinolin-4-yl)-2-methyl-1H-benzo[d]imidazole-4-carboxamide (**22**) (5.77 g, 77% over 2 steps). *m/z* calcd for $C_{24}H_{15}F_2N_6O$ $[M+H]^+$ 441.1, found ESI MS *m/z* 441.1 $[M+H]^+$.

4-(1-(5,8-difluoroquinolin-4-yl)-2-methyl-4-(4H-1,2,4-triazol-3-yl)-1H-benzo[d]imidazol-6-yl)picolinonitrile ((*rac*)-14). **22** (5.77 g, 13.1 mmol) was suspended in 1,1-dimethoxy-N,N-dimethylmethanamine (87 mL, 655 mmol) and stirred at 110 °C for 16 h. The solution was cooled to ambient temperature, concentrated under reduced pressure, and dried under vacuum overnight. The resulting residue was brought up in acetic acid (80 mL) and added dropwise over 20 min into a solution of hydrazine (1.23 mL, 39.3 mmol) in AcOH (50 mL). The mixture was stirred at 65 °C for 30 minutes. The mixture was slowly cool down to room temperature and allowed to recrystallize for o/n. The solid was isolated via filtration. The crude product was purified by silica gel column chromatography, eluting with 0-15% (1% NH_4OH in MeOH) in DCM to afford 4-(1-(5,8-difluoroquinolin-4-yl)-2-methyl-4-(4H-1,2,4-triazol-3-yl)-1H-benzo[d]imidazol-6-yl)picolinonitrile ((*rac*)-**14**) (4.10 g, 68%). *m/z* calcd for $C_{25}H_{15}F_2N_8$ $[M+H]^+$ 465.1, found ESI MS *m/z* 465.1 $[M+H]^+$.

(*P*)-4-(1-(5,8-difluoroquinolin-4-yl)-2-methyl-4-(4H-1,2,4-triazol-3-yl)-1H-benzo[d]imidazol-6-yl)picolinonitrile ((*P*)-14) and (*M*)-4-(1-(5,8-difluoroquinolin-4-yl)-2-methyl-4-(4H-1,2,4-triazol-3-yl)-1H-benzo[d]imidazol-6-yl)picolinonitrile ((*M*)-14). The atropisomers of (*rac*)-**14** were separated using SFC CHIRALPAK OJ-H 5uM 21x250mm column eluting with 30% MeOH/CO_2 at 60 mL/min (multiple injections). The appropriate fractions were pooled and concentrated to afford (*P*)-**14** (first eluting peak) and (*M*)-**14** (second eluting peak). ^{1}H NMR (400 MHz, $CDCl_3$) δ 13.33 (s, 1H), 9.32 (d, J = 4.4 Hz, 1H), 8.70 (dd, J = 5.2, 0.8 Hz, 1H), 8.50 – 8.47 (m, 1H), 8.16 (d, J = 0.8 Hz, 1H), 7.88 (dd, J = 2.0, 0.8 Hz, 1H), 7.75 (dd, J = 5.2, 1.9 Hz, 1H), 7.65 (d, J = 4.5 Hz, 1H), 7.56 (td, J = 9.0, 4.2 Hz, 1H), 7.30 – 7.22 (m, 1H), 7.20 (d, J = 1.8 Hz, 1H), 2.54 (s, 3H). *m/z* calcd for $C_{25}H_{15}F_2N_8$ $[M+H]^+$ 465.1, found ESI MS *m/z* 465.1 $[M+H]^+$.

3. CHARACTERIZATION OF FINAL COMPOUNDS

*All final compounds were isolated as TFA salts and were determined to be at least 95% pure by LC analysis.

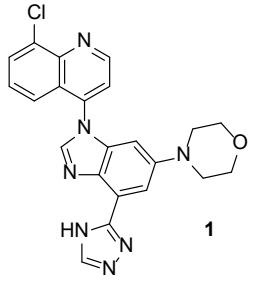

1

4-(1-(8-chloroquinolin-4-yl)-4-(4H-1,2,4-triazol-3-yl)-1H-benzo[d]imidazol-6-yl)morpholine. ^{1}H NMR (400 MHz, DMSO-d6) δ 9.30 (d, J = 4.6 Hz, 1H), 9.12 (s, 1H), 8.50 (s, 1H), 8.14 (dd, J = 7.4, 1.3 Hz, 1H), 8.04 (d, J = 4.6 Hz, 1H), 7.81 (d, J = 2.3 Hz, 1H), 7.69 – 7.62 (m, 1H), 7.61 – 7.56 (m, 1H), 6.87 (d, J = 2.3 Hz, 1H), 3.69 (t, J = 4.8 Hz, 4H), 3.13 – 3.07 (m, 4H). *m/z* calcd for $C_{22}H_{19}ClN_7O$ $[M+H]^+$ 432.1, found ESI MS *m/z* 432.1 $[M+H]^+$.

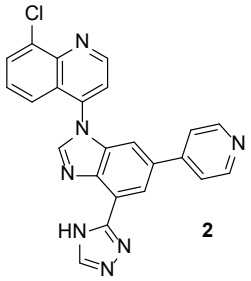

2

8-chloro-4-(6-(pyridin-4-yl)-4-(4H-1,2,4-triazol-3-yl)-1H-benzo[d]imidazol-1-yl)quinoline. ^{1}H NMR (400 MHz, DMSO-d6) δ 9.34 – 9.26 (m, 1H), 9.02 (s, 1H), 8.77 – 8.71 (m, 2H), 8.48 (d, J = 1.7 Hz, 1H), 8.39 (s, 1H), 8.14 – 8.06 (m, 4H), 7.99 (d, J = 1.7 Hz, 1H), 7.63 (dd, J = 8.5, 7.4 Hz, 1H), 7.55 (dd, J = 8.5, 1.3 Hz, 1H). *m/z* calcd for $C_{23}H_{15}ClN_7$ $[M+H]^+$ 424.1, found ESI MS *m/z* 424.1 $[M+H]^+$.

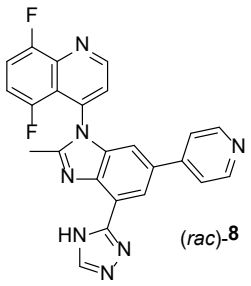

(*rac*)-**8**

5,8-difluoro-4-(2-methyl-6-(pyridin-4-yl)-4-(4H-1,2,4-triazol-3-yl)-1H-benzo[d]imidazol-1-yl)quinoline. ^{1}H NMR (400 MHz, DMSO-d6) δ 9.33 (d, J = 4.5 Hz, 1H), 8.78 – 8.73 (m, 2H), 8.46 (dd, J = 1.8, 0.6 Hz, 1H), 8.23 – 8.16 (m, 2H), 8.09 (d, J = 4.5 Hz, 1H), 7.91 (dd, J = 1.8, 0.6 Hz, 1H), 7.79 (td, J = 9.5, 4.2 Hz, 1H), 7.47 (ddd, J = 12.3, 8.7, 3.8 Hz, 1H), 2.50 (s, 3H). *m/z* calcd for $C_{24}H_{16}F_2N_7$ $[M+H]^+$ 440.1, found ESI MS *m/z* 440.1 $[M+H]^+$.

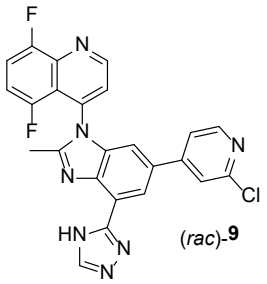

(*rac*)-**9**

4-(6-(2-chloropyridin-4-yl)-2-methyl-4-(4H-1,2,4-triazol-3-yl)-1H-benzo[d]imidazol-1-yl)-5,8-difluoroquinoline. ^{1}H NMR (400 MHz, DMSO-d6) δ 9.36 (d, J = 4.5 Hz, 1H), 8.51 (s, 1H), 8.41 (dd, J = 5.3, 0.6 Hz, 1H), 8.38 (dd, J = 1.8, 0.9 Hz, 1H), 8.11 (d, J = 4.6 Hz, 1H), 7.88 – 7.75 (m, 4H), 7.50 (ddd, J = 12.3, 8.7, 3.8 Hz, 1H), 2.53 (d, J = 1.0 Hz, 3H). *m/z* calcd for $C_{24}H_{15}F_2N_7$ $[M+H]^+$ 474.1, found ESI MS *m/z* 474.1 $[M+H]^+$.

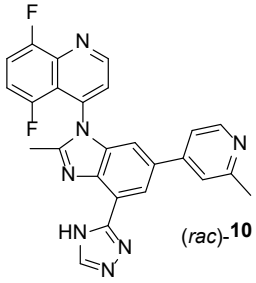

(*rac*)-**10**

5,8-difluoro-4-(2-methyl-6-(2-methylpyridin-4-yl)-4-(4H-1,2,4-triazol-3-yl)-1H-benzo[d]imidazol-1-yl)quinoline. ^{1}H NMR (400 MHz, DMSO-d6) δ 9.34 (d, J = 4.5 Hz, 1H), 8.70 (dd, J = 6.4, 0.6 Hz, 1H), 8.48 (d, J = 1.8 Hz, 1H), 8.44 (s, 1H), 8.25 (d, J = 1.9 Hz, 1H), 8.15 (dd, J = 6.3, 2.0 Hz, 1H), 8.10 (d, J = 4.5 Hz, 1H), 7.90 (d, J = 1.8 Hz, 1H), 7.79 (ddd, J = 10.0, 8.8, 4.2 Hz, 1H), 7.47 (ddd, J = 12.3, 8.8, 3.8 Hz, 1H), 2.67 (s, 3H), 2.48 (s, 3H). *m/z* calcd for $C_{25}H_{18}F_2N_7$ $[M+H]^+$ 454.1, found ESI MS *m/z* 454.2 $[M+H]^+$.

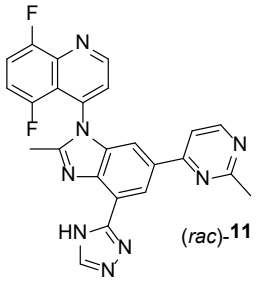

(*rac*)-**11**

5,8-difluoro-4-(2-methyl-6-(2-methylpyrimidin-4-yl)-4-(4H-1,2,4-triazol-3-yl)-1H-benzo[d]imidazol-1-yl)quinoline. ^{1}H NMR (400 MHz, DMSO-d6) δ 9.37 (d, J = 4.5 Hz, 1H), 8.95 (d, J = 1.6 Hz, 1H), 8.67 (d, J = 5.5 Hz, 1H), 8.52 (s, 1H), 8.14 (d, J = 4.5 Hz, 1H), 8.06 (d, J = 1.6 Hz, 1H), 7.90 (dd, J = 5.5, 0.7 Hz, 1H), 7.82 (ddd, J = 10.0, 8.8, 4.2 Hz, 1H), 7.50 (ddd, J = 12.4, 8.8, 3.8 Hz, 1H), 2.66 (s, 3H), 2.55 (s, 3H). *m/z* calcd for $C_{24}H_{17}F_2N_8$ $[M+H]^+$ 455.1, found ESI MS *m/z* 455.2 $[M+H]^+$.

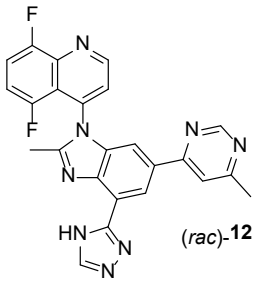

(*rac*)-**12**

5,8-difluoro-4-(2-methyl-6-(6-methylpyrimidin-4-yl)-4-(4H-1,2,4-triazol-3-yl)-1H-benzo[d]imidazol-1-yl)quinoline. ^{1}H NMR (400 MHz, DMSO-d6) δ 9.39 (d, J = 4.5 Hz, 1H), 9.05 (d, J = 1.3 Hz, 1H), 8.97 (d, J = 1.6 Hz, 1H), 8.58 (s, 1H), 8.16 (d, J = 4.5 Hz, 1H), 8.06 (d, J = 1.6 Hz, 1H), 8.01 (dd, J = 1.3, 0.6 Hz, 1H), 7.83 (ddd, J = 10.0, 8.8, 4.2 Hz, 1H), 7.52 (ddd, J = 12.4, 8.8, 3.8 Hz, 1H), 2.57 (s, 3H), 2.47 (s, 3H). *m/z* calcd for $C_{24}H_{17}F_2N_8$ $[M+H]^+$ 455.1, found ESI MS *m/z* 455.2 $[M+H]^+$.

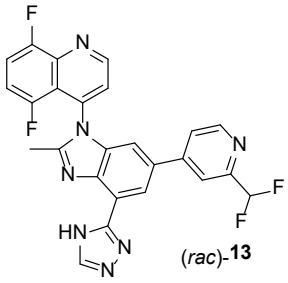

(*rac*)-**13**

4-(6-(2-(difluoromethyl)pyridin-4-yl)-2-methyl-4-(4H-1,2,4-triazol-3-yl)-1H-benzo[d]imidazol-1-yl)-5,8-difluoroquinoline. ^{1}H NMR (400 MHz, DMSO-d6) δ 9.34 (d, J = 4.5 Hz, 1H), 8.66 (dd, J = 5.2, 0.7 Hz, 1H), 8.53 (s, 1H), 8.41 (d, J = 1.7 Hz, 1H), 8.11 (d, J = 4.5 Hz, 1H), 7.97 (dd, J = 1.9, 0.7 Hz, 1H), 7.91

– 7.87 (m, 1H), 7.86 (d, J = 1.7 Hz, 1H), 7.79 (ddd, J = 10.0, 8.8, 4.2 Hz, 1H), 7.48 (ddd, J = 12.4, 8.8, 3.8 Hz, 1H), 6.96 (t, J = 54.8 Hz, 1H), 2.53 (s, 3H). ES/MS *m/z* 490.1 $(M+H)^+$.

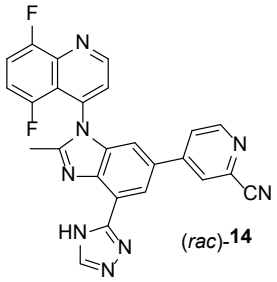

(*rac*)-**14**

4-(1-(5,8-difluoroquinolin-4-yl)-2-methyl-4-(4H-1,2,4-triazol-3-yl)-1H-benzo[d]imidazol-6-yl)picolinonitrile. ^{1}H NMR (400 MHz, DMSO-d6) δ 9.34 (d, J = 4.5 Hz, 1H), 8.71 (dd, J = 5.3, 0.8 Hz, 1H), 8.50 (s, 1H), 8.43 (d, J = 1.7 Hz, 1H), 8.39 (dd, J = 2.0, 0.8 Hz, 1H), 8.11 – 8.07 (m, 2H), 7.87 (d, J = 1.7 Hz, 1H), 7.79 (ddd, J = 10.1, 8.8, 4.3 Hz, 1H), 7.48 (ddd, J = 12.3, 8.8, 3.8 Hz, 1H), 2.52 (s, 3H). *m/z* calcd for $C_{25}H_{15}F_2N_8$ $[M+H]^+$ 465.1, found ESI MS *m/z* 465.1 $[M+H]^+$.

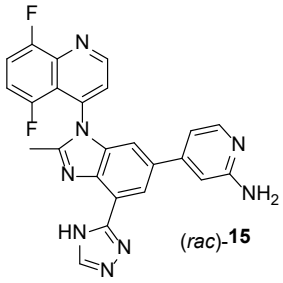

(*rac*)-**15**

4-(1-(5,8-difluoroquinolin-4-yl)-2-methyl-4-(4H-1,2,4-triazol-3-yl)-1H-benzo[d]imidazol-6-yl)pyridin-2-amine. ^{1}H NMR (400 MHz, DMSO-d6) δ 9.32 (d, J = 4.5 Hz, 1H), 8.30 (d, J = 1.3 Hz, 1H), 8.07 (d, J = 4.7 Hz, 1H), 7.89 (d, J = 6.8 Hz, 1H), 7.87 – 7.74 (m, 4H), 7.69 (s, 1H), 7.52 – 7.36 (m, 1H), 7.26 – 7.19 (m, 2H), 2.52 (s, 3H). *m/z* calcd for $C_{24}H_{17}F_2N_8$ $[M+H]^+$ 455.1, found ESI MS *m/z* 455.2 $[M+H]^+$.

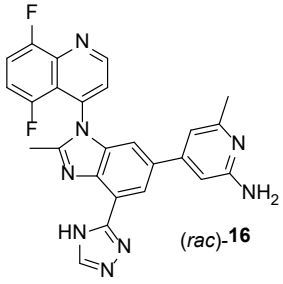

(*rac*)-**16**

4-(1-(5,8-difluoroquinolin-4-yl)-2-methyl-4-(4H-1,2,4-triazol-3-yl)-1H-benzo[d]imidazol-6-yl)-6-methylpyridin-2-amine. ^{1}H NMR (400 MHz, DMSO-d6) δ 9.33 (d, J = 4.5 Hz, 1H), 8.30 (d, J = 1.7 Hz,

1H), 8.08 (d, J = 4.5 Hz, 1H), 7.84 – 7.75 (m, 1H), 7.64 (s, 1H), 7.60 (s, 2H), 7.47 (ddd, J = 12.3, 8.8, 3.8 Hz, 1H), 7.10 (s, 1H), 7.06 (s, 1H), 2.45 (s, 3H), 2.39 (s, 3H). ES/MS *m/z* 469.2 $(M+H)^+$. *m/z* calcd for $C_{25}H_{19}F_2N_8$ $[M+H]^+$ 469.2, found ESI MS *m/z* 469.2 $[M+H]^+$.

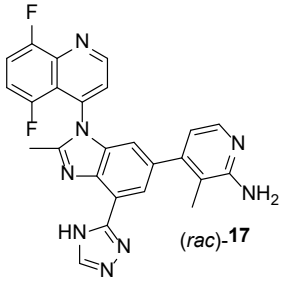

(*rac*)-**17**

4-(1-(5,8-difluoroquinolin-4-yl)-2-methyl-4-(4H-1,2,4-triazol-3-yl)-1H-benzo[d]imidazol-6-yl)-3-methylpyridin-2-amine. ^{1}H NMR (400 MHz, DMSO-d6) δ 9.28 (d, J = 4.5 Hz, 1H), 8.06 (d, J = 4.5 Hz, 1H), 7.88 (d, J = 1.6 Hz, 1H), 7.84 – 7.74 (m, 4H), 7.47 (ddd, J = 12.3, 8.8, 3.9 Hz, 1H), 7.29 (s, 1H), 6.83 (d, J = 6.6 Hz, 1H), 1.99 (s, 3H). *m/z* calcd for $C_{25}H_{19}F_2N_8$ $[M+H]^+$ 469.2, found ESI MS *m/z* 469.2 $[M+H]^+$.

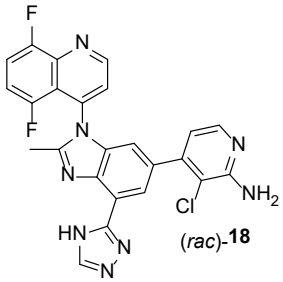

(*rac*)-**18**

3-chloro-4-(1-(5,8-difluoroquinolin-4-yl)-2-methyl-4-(4H-1,2,4-triazol-3-yl)-1H-benzo[d]imidazol-6-yl)pyridin-2-amine. ^{1}H NMR (400 MHz, DMSO-d6) δ 9.30 (d, J = 4.5 Hz, 1H), 8.47 (s, 1H), 8.10 (d, J = 4.5 Hz, 1H), 8.07 (d, J = 1.6 Hz, 1H), 7.90 (d, J = 5.6 Hz, 1H), 7.78 (td, J = 9.4, 4.2 Hz, 1H), 7.49 (ddd, J = 12.4, 8.9, 3.8 Hz, 1H), 7.41 (d, J = 1.6 Hz, 1H), 6.70 (d, J = 5.6 Hz, 1H), 2.55 (s, 3H). ES/MS *m/z* 489.2 $(M+H)^+$. *m/z* calcd for $C_{24}H_{16}ClF_2N_8$ $[M+H]^+$ 489.1, found ESI MS *m/z* 489.2 $[M+H]^+$.

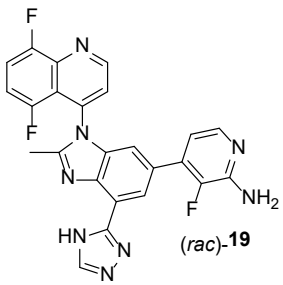

(*rac*)-**19**

4-(1-(5,8-difluoroquinolin-4-yl)-2-methyl-4-(4H-1,2,4-triazol-3-yl)-1H-benzo[d]imidazol-6-yl)-3-fluoropyridin-2-amine. ^{1}H NMR (400 MHz, DMSO-d6) δ 9.31 (d, J = 4.5 Hz, 1H), 8.41 (br s, 1H), 8.22 (s, 1H), 8.09 (d, J = 4.5 Hz, 1H), 7.78 (td, J = 9.5, 4.2 Hz, 1H), 7.74 (dd, J = 6.2, 0.9 Hz, 1H), 7.52 (s, 1H), 7.47 (ddd, J = 12.3, 8.8, 3.8 Hz, 1H), 6.84 (br s, 1H), 2.51 (s, 3H). *m/z* calcd for $C_{24}H_{16}F_3N_8$ $[M+H]^+$ 473.1, found ESI MS *m/z* 473.2 $[M+H]^+$.

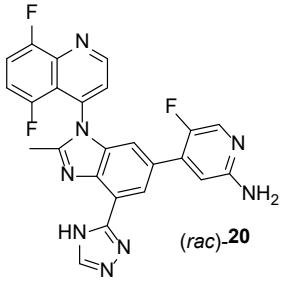

(*rac*)-**20**

4-(1-(5,8-difluoroquinolin-4-yl)-2-methyl-4-(4H-1,2,4-triazol-3-yl)-1H-benzo[d]imidazol-6-yl)-5-fluoropyridin-2-amine. ^{1}H NMR (400 MHz, DMSO-d6) δ 9.31 (d, J = 4.5 Hz, 1H), 8.42 (br s, 1H), 8.17 (t, J = 1.8 Hz, 1H), 8.10 (s, 1H), 8.09 (s, 1H), 7.83 – 7.75 (m, 1H), 7.53 – 7.43 (m, 2H), 6.82 (d, J = 6.0 Hz, 1H), 2.50 (s, 3H). *m/z* calcd for $C_{24}H_{16}F_3N_8$ $[M+H]^+$ 473.1, found ESI MS *m/z* 473.2 $[M+H]^+$.

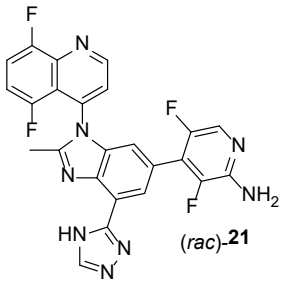

(*rac*)-**21**

4-(1-(5,8-difluoroquinolin-4-yl)-2-methyl-4-(4H-1,2,4-triazol-3-yl)-1H-benzo[d]imidazol-6-yl)-3,5-difluoropyridin-2-amine. ^{1}H NMR (400 MHz, DMSO-d6) δ 9.30 (d, J = 4.5 Hz, 1H), 8.47 (s, 1H), 8.10 (d, J = 4.6 Hz, 1H), 8.06 (d, J = 1.4 Hz, 1H), 7.87 (t, J = 0.6 Hz, 1H), 7.82 – 7.75 (m, 1H), 7.52 – 7.44 (m, 2H), 2.55 (s, 3H). *m/z* calcd for $C_{24}H_{15}F_4N_8$ $[M+H]^+$ 491.1, found ESI MS *m/z* 491.1 $[M+H]^+$.

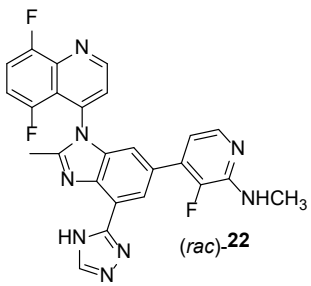

(*rac*)-**22**

4-(1-(5,8-difluoroquinolin-4-yl)-2-methyl-4-(4H-1,2,4-triazol-3-yl)-1H-benzo[d]imidazol-6-yl)-3-fluoro-N-methylpyridin-2-amine. ^{1}H NMR (400 MHz, DMSO-d6) δ 9.31 (d, J = 4.5 Hz, 1H), 8.47 (s, 1H), 8.23 (t, J = 1.6 Hz, 1H), 8.10 (d, J = 4.5 Hz, 1H), 7.83 – 7.75 (m, 2H), 7.53 (s, 1H), 7.48 (ddd, J = 12.3, 8.8, 3.8 Hz, 1H), 6.74 (t, J = 5.6 Hz, 1H), 2.87 (s, 3H), 2.53 (s, 3H). *m/z* calcd for $C_{25}H_{18}F_3N_8$ $[M+H]^+$ 487.2, found ESI MS *m/z* 487.2 $[M+H]^+$.

4. PI3K BIOCHEMICAL ASSAYS. Enzymatic activity of the class I PI3K isoforms was measured using a time resolved fluorescence resonance energy transfer (TR-FRET) assay that monitors formation of the product 3,4,5-inositol triphosphate molecule (PIP3). Human full length p110α and human p110δ catalytic subunits were co-expressed with the p85α regulatory subunit and purified as heterodimers. Human full length p110γ was expressed and purified without a regulatory subunit. PI3Kβ was purchased from Millipore (Billerica, MA) (item 14-603, lot 1994929-B). All assay reagents and buffers for the TR-FRET assay were purchased from Millipore (Dundee, Ireland) (item 33-036, lot 1812413). PI3K isoforms were assayed under initial rate conditions (2 x K_m ATP, 10 uM PIP2) at the following concentrations for each isoform: PI3K α, β, at 100 pM, δ at 20 pM, and PI3Kγ at 5 nM. After an assay reaction time of 30 minutes at 25 °C, reactions were terminated with a final concentration of 10 mM EDTA, 10 nM labeled-PIP3, and 35 nM Europium labeled GRP-1 detector protein before reading TR-FRET on an Envision plate reader (Ex: 340 nm; Em: 615/665 nm). Data were normalized based on a positive (1 μM wortmannin) and negative (0.5% DMSO) control and IC_{50} values were calculated from the fit of the dose-response curves to a four-parameter equation. All IC_{50} values represent geometric mean values of a minimum of four determinations.

5. EC_{50} (pAKT1), PI3Kβ. Inhibition of pAKT1 S^{473} was assessed PC3, LNCaP, MDA-MB-415, ZR-75-1 and A498 cell lines were cultured according to ATCC guidelines to log phase growth and seeded in 96 well microtiter plates at 20,000 cells per well. The compound was applied from 1.0 μM to 0.0005 μM along a 36-point gradient and incubated 2 hours at 37 °C 100%RH. Cells were lysed (Cell Signaling Technology #9803 with 1mM PMSF #8553) and assessed for AKT1 and pAKT1 S^{473} quantitatively by Mesoscale Diagnostics (MSD) kits K150MOD and K150MND, respectively. Data determined from the ratio of Units pAKT1 S^{473} per nanogram total AKT1.

6. HEPATOCYTE METABOLIC STABILITY ASSAY. Cryopreserved hepatocytes were thawed according to the protocol provided by the manufacturer and resuspended in KHB buffer at a at a final test compound concentration of 1 μM (1 million cells/mL). Incubations were allowed to proceed with gentle

rocking in a 37°C cell culture incubator with a 5% carbon dioxide/95% air atmosphere and saturating humidity. Aliquots were taken from each well at 0, 75, 110, 180 and 250 min and quenched, processed and analyzed by ultra-high pressure liquid chromatography (UHPLC) with high resolution mass (HRMS) detection. Half-lives of parent compounds were calculated using linear regression of log-transformed percent remaining over time. Predicted clearances were calculated using the well-stirred liver model.

7. CACO-2 PERMEABILITY. Caco-2 cells were maintained in Dulbecco's Modification of Eagle's Medium (DMEM) with sodium pyruvate, Glutmax supplemented with 1% Pen/Strep, 1% NEAA and 10% fetal bovine serum in an incubator set at 37ºC, 90% humidity and 5% CO_2. Caco-2 cells between passage 62 and 72 were seeded at 2100 cells / well and were grown to confluence over at least 21-days on 24 well PET (polyethylene-terephthalate) plates (BD Biosciences). Experiments are run using a new HBSS donor buffer from Invitrogen containing additional 10mM HEPES, 15mM Glucose with pH adjusted to pH 6.5. The receiver well uses HBSS buffer supplemented with 1% BSA and the pH adjusted to pH 7.4. After an initial equilibration with transport buffer, TEER values are read to test membrane integrity. The experiment is started by the addition of buffers containing test compounds and 100 µl of solution is taken at 1 and 2 hrs from the receiver compartment. Removed buffer is replaced with fresh buffer and a correction is applied to all calculations for the removed material. Each compound (10 µM) is tested in 2 separate replicate wells for each condition. All samples are immediately collected into 400 µl 100% acetonitrile acid to precipitate protein and stabilize test compounds. Cells are dosed on the apical or basolateral side to determine forward (A to B) and reverse (B to A) permeability. Permeability through a cell free trans-well is also determined as a measure of cellular permeability through the membrane and non-specific binding. To test for non-specific binding and compound instability the total amount of drug is quantitated at the end of the experiment and compared to the material present in the original dosing solution as a percent recovery. Samples are analyzed by LC/MS/MS.

The apparent permeability, Papp, and % recovery were calculated as follows:

$$\mathbf{P_{app} = (\mathit{d}R/\mathit{d}t) \times V_r/(A \times D_0)}$$

$$\mathbf{\% \ Recovery = 100 \times ((V_r \times R_{120}) + (V_d \times D_{120}))/ (V_d \times D_0)}$$

Where,

dR/d*t* is the slope of the cumulative concentration in the receiver compartment versus time in µM/s based on receiver concentrations measured at 60 and 120 minutes.

$\mathbf{V_r}$ and $\mathbf{V_d}$ is the volume in the receiver and donor compartment in cm^3, respectively.

A is the area of the cell monolayer (0.33 cm^2).

$\mathbf{D_0}$ and $\mathbf{D_{120}}$ is the measured donor concentration at the beginning and end of the experiment, respectively.

$\mathbf{R_{120}}$ is the receiver concentration at the end of the experiment (120 minutes).

8. PHARMACOKINETICS. Pharmacokinetic studies were performed in naive male prague-Dawley rats, male Beagle dogs, male Cynomolgus monkeys and male Rhesus monkeys (three animals per dosing route) following federal and Institutional Animal Care and Use Committee (IACUC) guidelines. The intravenous administration was dosed via infusion over 30 min and oral dosing was administered by gavage. Blood samples were collected over a 24 h period post-dose into Vacutainer tubes containing EDTA-K2. Plasma was isolated, and the concentration of the test compound in plasma was determined with ESI+ LC/MS/MS after protein precipitation with acetonitrile. Non-compartmental pharmacokinetic analysis was performed on the plasma concentration-time data. The intravenous doses of were formulated in 40% PEG 300 and 60% water. The oral doses were formulated in 40% PEG 300 and 60% water.

9. OCULAR ASSESSMENT. The toxicology profile of *P*-(**14**) was evaluated in a 7 day repeat dose dog study. In addition to routine ophthalmic exams, detailed ocular assessments of electroretinography (ERG) and optical coherence tomography (OCT) were included. Male beagle dogs (3/group) were dosed daily with *P*-(**14**) at 0 (vehicle), 10, 40 and 100 mg/kg/day. Based on poor tolerability, high dose animals were euthanized after the second dose on Day 2. Dosing was suspended in the 40 mg/kg/day group on Day 4 and resumed on Day 5 at 30 mg/kg/day. Ocular toxicity, characterized by both structural and functional effects, was present at the low and mid dose levels and was considered likely irreversible. Clinical observations indicated decreased response to visual stimuli, dilated pupils, red conjunctiva and ocular discharge in all animals beginning on Day 4 through the end of the study.

Ophthalmic evaluations, ERG and OCT were conducted before the beginning of the study (pre-dose) and on Day 6. ERG assessment following dark-adaptation indicated that all dogs in the 10 and 40/30 mg/kg/day groups had no response to single light flashes of 0.01, 0.06, or 2.5 cd·s/m^2. Ophthalmic evaluation (slit lamp biomicroscope/indirect ophthalmoscopy) revealed decreased tapetum in 2/3 dogs at 10 mg/kg/day with complete loss of tapetum in 3/3 dogs and retinal detachment in 2/3 dogs at 40/30 mg/kg/day.

OCT imaging confirmed the tapetal changes and retinal detachment. Additional effects noted with OCT included photoreceptor layers appearing as an indistinct single hyper-reflective band and swelling of the optic nerve in the 10 and 40/30 mg/kg/day dose groups. Microscopically, retinal degeneration/necrosis and choroidal inflammation were noted in all animals, including animals in the 100 mg/kg/day dose group.

Table S3. Toxicokinetic exposure margins

	10 mg/kg QD	**40/30 mg/kg QD**	**50 mg/kg BID***
$AUC_{0\text{-}24h}$ (µM·hr)	49	220	256
C_{max} (µM)	4.4	12.7	14.5
AUC Margin**	1.8x	8.1x	9.5x
C_{max} Margin**	2.9x	8.5x	9.7x

*2^{nd} dose given 8 hours after 1^{st}

**Calculated after single dose, using predicted human $AUC_{0\text{-}24}$= 27 µM·h , C_{max} = 1.5 µM

Figure S1. Functional ERG response of the retina to increasing light stimulus

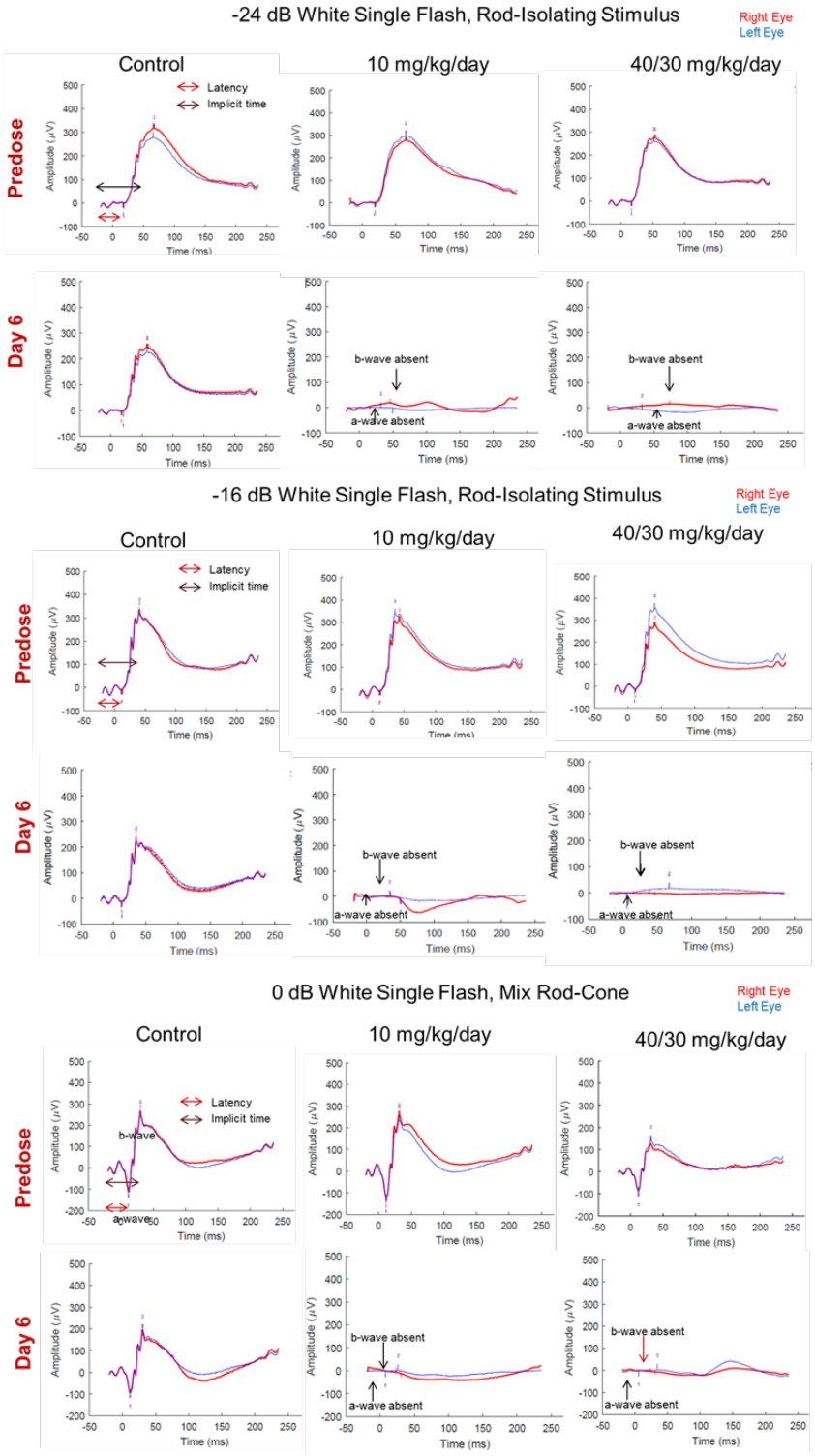

Figure S2. OCT images showing ocular effects at 10 mg/kg/day

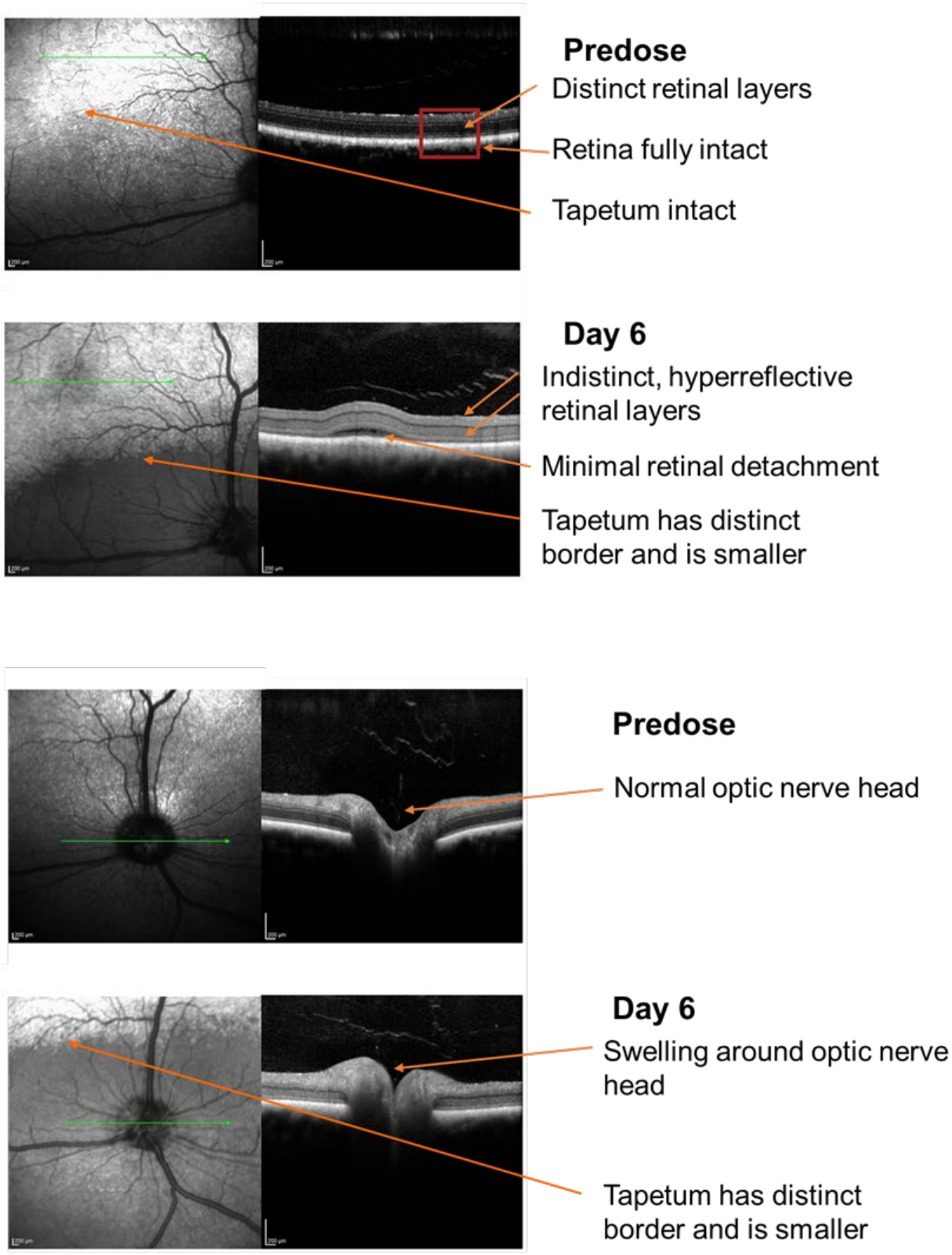

Figure S3. OCT images showing ocular effects at 40/30 mg/kg/day

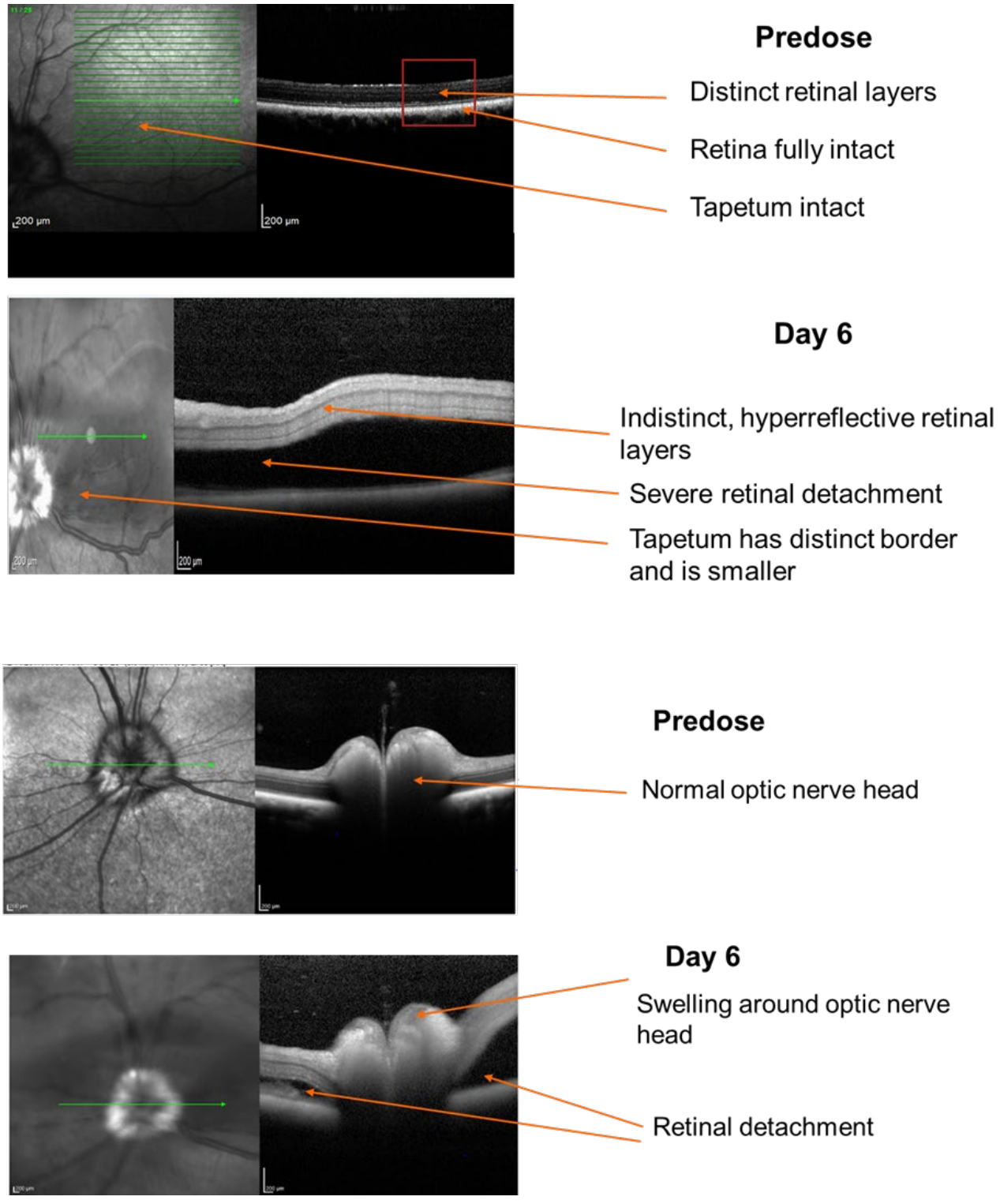

10. KINASE SELECTIVITY PROFILE OF (P-14)

Compound (*P*)-**14** was screened at 10 μM in the KINOMEscan® (DiscoverX, San Diego, CA) assay, and the results for the primary screen binding interactions are reported as "percent control", where lower numbers indicate stronger hits in the matrix. For the kinase selectivity profile of (*P*)-**19**, see *J. Med. Chem.* **2018**, *61*, 6858-6868.

Figure S4. Protein and lipid kinase selectivity profiles of (*P*)-**14** using the DiscoverX KINOMEscan® platform at a compound concentration of 10 μM. PI3Kβ highlighted with a blue circle. Image generated using TREEspot™ Software Tool and reprinted with permission from KINOMEscan®, a division of DiscoverX Corporation, © DISCOVERX CORPORATION 2010.

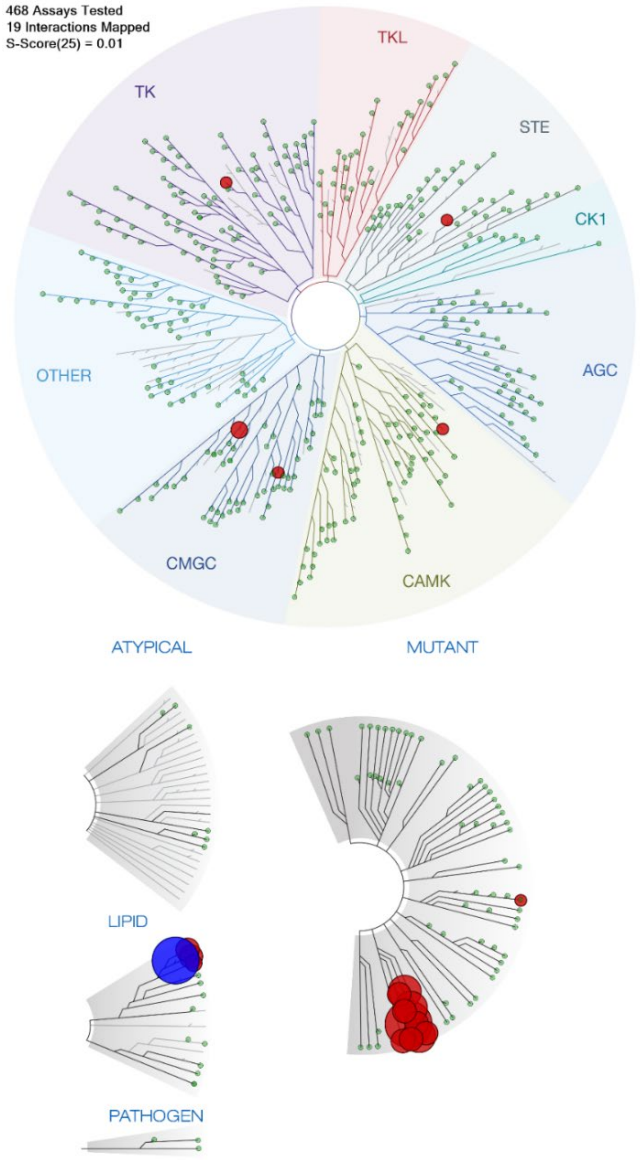

Table S4. Dose responses (K_d values) of (*P*)-14 using the DiscoverX KINOMEscan® platform.

DiscoverX Gene Symbol	K_d (nM)
CDK7	1,300
HIPK4	5,700
MEK5	5,200
PIK3CB	0.49

Table S5. DiscoverX KINOMEscan primary screen data of compound (*P*)-14 at 10 μM

DiscoverX Gene Symbol	Entrez Gene Symbol	Percent Control	Compound Concentration (nM)
AAK1	AAK1	95	10000
ABL1(E255K)-phosphorylated	ABL1	92	10000
ABL1(F317I)-nonphosphorylated	ABL1	96	10000
ABL1(F317I)-phosphorylated	ABL1	87	10000
ABL1(F317L)-nonphosphorylated	ABL1	88	10000
ABL1(F317L)-phosphorylated	ABL1	100	10000
ABL1(H396P)-nonphosphorylated	ABL1	74	10000
ABL1(H396P)-phosphorylated	ABL1	100	10000
ABL1(M351T)-phosphorylated	ABL1	100	10000
ABL1(Q252H)-nonphosphorylated	ABL1	67	10000
ABL1(Q252H)-phosphorylated	ABL1	100	10000
ABL1(T315I)-nonphosphorylated	ABL1	98	10000
ABL1(T315I)-phosphorylated	ABL1	100	10000
ABL1(Y253F)-phosphorylated	ABL1	93	10000
ABL1-nonphosphorylated	ABL1	69	10000
ABL1-phosphorylated	ABL1	85	10000
ABL2	ABL2	100	10000
ACVR1	ACVR1	92	10000
ACVR1B	ACVR1B	98	10000
ACVR2A	ACVR2A	69	10000
ACVR2B	ACVR2B	80	10000
ACVRL1	ACVRL1	100	10000
ADCK3	CABC1	79	10000
ADCK4	ADCK4	93	10000
AKT1	AKT1	91	10000
AKT2	AKT2	97	10000
AKT3	AKT3	97	10000
ALK	ALK	91	10000
ALK(C1156Y)	ALK	100	10000
ALK(L1196M)	ALK	92	10000

AMPK-alpha1	PRKAA1	87	10000
AMPK-alpha2	PRKAA2	94	10000
ANKK1	ANKK1	100	10000
ARK5	NUAK1	97	10000
ASK1	MAP3K5	100	10000
ASK2	MAP3K6	91	10000
AURKA	AURKA	76	10000
AURKB	AURKB	73	10000
AURKC	AURKC	92	10000
AXL	AXL	90	10000
BIKE	BMP2K	97	10000
BLK	BLK	96	10000
BMPR1A	BMPR1A	91	10000
BMPR1B	BMPR1B	94	10000
BMPR2	BMPR2	90	10000
BMX	BMX	79	10000
BRAF	BRAF	95	10000
BRAF(V600E)	BRAF	97	10000
BRK	PTK6	92	10000
BRSK1	BRSK1	73	10000
BRSK2	BRSK2	87	10000
BTK	BTK	69	10000
BUB1	BUB1	96	10000
CAMK1	CAMK1	82	10000
CAMK1B	PNCK	94	10000
CAMK1D	CAMK1D	91	10000
CAMK1G	CAMK1G	100	10000
CAMK2A	CAMK2A	90	10000
CAMK2B	CAMK2B	80	10000
CAMK2D	CAMK2D	98	10000
CAMK2G	CAMK2G	100	10000
CAMK4	CAMK4	100	10000
CAMKK1	CAMKK1	92	10000
CAMKK2	CAMKK2	100	10000
CASK	CASK	91	10000
CDC2L1	CDK11B	93	10000
CDC2L2	CDC2L2	66	10000
CDC2L5	CDK13	87	10000
CDK11	CDK19	84	10000
CDK2	CDK2	84	10000
CDK3	CDK3	100	10000

CDK4	CDK4	93	10000
CDK4-cyclinD1	CDK4	76	10000
CDK4-cyclinD3	CDK4	98	10000
CDK5	CDK5	86	10000
CDK7	CDK7	78	10000
CDK8	CDK8	94	10000
CDK9	CDK9	93	10000
CDKL1	CDKL1	85	10000
CDKL2	CDKL2	99	10000
CDKL3	CDKL3	87	10000
CDKL5	CDKL5	99	10000
CHEK1	CHEK1	100	10000
CHEK2	CHEK2	89	10000
CIT	CIT	82	10000
CLK1	CLK1	100	10000
CLK2	CLK2	99	10000
CLK3	CLK3	90	10000
CLK4	CLK4	85	10000
CSF1R	CSF1R	89	10000
CSF1R-autoinhibited	CSF1R	90	10000
CSK	CSK	86	10000
CSNK1A1	CSNK1A1	85	10000
CSNK1A1L	CSNK1A1L	80	10000
CSNK1D	CSNK1D	72	10000
CSNK1E	CSNK1E	97	10000
CSNK1G1	CSNK1G1	94	10000
CSNK1G2	CSNK1G2	84	10000
CSNK1G3	CSNK1G3	100	10000
CSNK2A1	CSNK2A1	91	10000
CSNK2A2	CSNK2A2	84	10000
CTK	MATK	85	10000
DAPK1	DAPK1	93	10000
DAPK2	DAPK2	87	10000
DAPK3	DAPK3	86	10000
DCAMKL1	DCLK1	75	10000
DCAMKL2	DCLK2	64	10000
DCAMKL3	DCLK3	100	10000
DDR1	DDR1	86	10000
DDR2	DDR2	96	10000
DLK	MAP3K12	100	10000
DMPK	DMPK	99	10000

DMPK2	CDC42BPG	93	10000
DRAK1	STK17A	97	10000
DRAK2	STK17B	99	10000
DYRK1A	DYRK1A	95	10000
DYRK1B	DYRK1B	66	10000
DYRK2	DYRK2	98	10000
EGFR	EGFR	100	10000
EGFR(E746-A750del)	EGFR	99	10000
EGFR(G719C)	EGFR	92	10000
EGFR(G719S)	EGFR	99	10000
EGFR(L747-E749del, A750P)	EGFR	100	10000
EGFR(L747-S752del, P753S)	EGFR	82	10000
EGFR(L747-T751del,Sins)	EGFR	91	10000
EGFR(L858R)	EGFR	94	10000
EGFR(L858R,T790M)	EGFR	100	10000
EGFR(L861Q)	EGFR	96	10000
EGFR(S752-I759del)	EGFR	96	10000
EGFR(T790M)	EGFR	91	10000
EIF2AK1	EIF2AK1	96	10000
EPHA1	EPHA1	95	10000
EPHA2	EPHA2	82	10000
EPHA3	EPHA3	65	10000
EPHA4	EPHA4	89	10000
EPHA5	EPHA5	92	10000
EPHA6	EPHA6	87	10000
EPHA7	EPHA7	97	10000
EPHA8	EPHA8	100	10000
EPHB1	EPHB1	100	10000
EPHB2	EPHB2	95	10000
EPHB3	EPHB3	90	10000
EPHB4	EPHB4	92	10000
EPHB6	EPHB6	100	10000
ERBB2	ERBB2	76	10000
ERBB3	ERBB3	48	10000
ERBB4	ERBB4	100	10000
ERK1	MAPK3	90	10000
ERK2	MAPK1	75	10000
ERK3	MAPK6	91	10000
ERK4	MAPK4	86	10000
ERK5	MAPK7	100	10000
ERK8	MAPK15	100	10000

ERN1	ERN1	99	10000
FAK	PTK2	100	10000
FER	FER	98	10000
FES	FES	100	10000
FGFR1	FGFR1	85	10000
FGFR2	FGFR2	100	10000
FGFR3	FGFR3	88	10000
FGFR3(G697C)	FGFR3	98	10000
FGFR4	FGFR4	89	10000
FGR	FGR	89	10000
FLT1	FLT1	95	10000
FLT3	FLT3	74	10000
FLT3(D835H)	FLT3	87	10000
FLT3(D835V)	FLT3	71	10000
FLT3(D835Y)	FLT3	68	10000
FLT3(ITD)	FLT3	84	10000
FLT3(ITD,D835V)	FLT3	65	10000
FLT3(ITD,F691L)	FLT3	50	10000
FLT3(K663Q)	FLT3	78	10000
FLT3(N841I)	FLT3	100	10000
FLT3(R834Q)	FLT3	96	10000
FLT3-autoinhibited	FLT3	79	10000
FLT4	FLT4	98	10000
FRK	FRK	96	10000
FYN	FYN	100	10000
GAK	GAK	84	10000
GCN2(Kin.Dom.2,S808G)	EIF2AK4	78	10000
GRK1	GRK1	83	10000
GRK2	ADRBK1	97	10000
GRK3	ADRBK2	89	10000
GRK4	GRK4	90	10000
GRK7	GRK7	99	10000
GSK3A	GSK3A	100	10000
GSK3B	GSK3B	73	10000
HASPIN	GSG2	85	10000
HCK	HCK	77	10000
HIPK1	HIPK1	75	10000
HIPK2	HIPK2	81	10000
HIPK3	HIPK3	76	10000
HIPK4	HIPK4	100	10000
HPK1	MAP4K1	93	10000

HUNK	HUNK	98	10000
ICK	ICK	65	10000
IGF1R	IGF1R	90	10000
IKK-alpha	CHUK	96	10000
IKK-beta	IKBKB	90	10000
IKK-epsilon	IKBKE	100	10000
INSR	INSR	87	10000
INSRR	INSRR	92	10000
IRAK1	IRAK1	98	10000
IRAK3	IRAK3	85	10000
IRAK4	IRAK4	100	10000
ITK	ITK	100	10000
JAK1(JH1domain-catalytic)	JAK1	89	10000
JAK1(JH2domain-pseudokinase)	JAK1	30	10000
JAK2(JH1domain-catalytic)	JAK2	81	10000
JAK3(JH1domain-catalytic)	JAK3	85	10000
JNK1	MAPK8	55	10000
JNK2	MAPK9	61	10000
JNK3	MAPK10	59	10000
KIT	KIT	40	10000
KIT(A829P)	KIT	65	10000
KIT(D816H)	KIT	81	10000
KIT(D816V)	KIT	68	10000
KIT(L576P)	KIT	47	10000
KIT(V559D)	KIT	40	10000
KIT(V559D,T670I)	KIT	48	10000
KIT(V559D,V654A)	KIT	94	10000
KIT-autoinhibited	KIT	95	10000
LATS1	LATS1	89	10000
LATS2	LATS2	84	10000
LCK	LCK	95	10000
LIMK1	LIMK1	80	10000
LIMK2	LIMK2	97	10000
LKB1	STK11	85	10000
LOK	STK10	86	10000
LRRK2	LRRK2	83	10000
LRRK2(G2019S)	LRRK2	100	10000
LTK	LTK	90	10000
LYN	LYN	92	10000
LZK	MAP3K13	99	10000
MAK	MAK	48	10000

MAP3K1	MAP3K1	73	10000
MAP3K15	MAP3K15	91	10000
MAP3K2	MAP3K2	94	10000
MAP3K3	MAP3K3	88	10000
MAP3K4	MAP3K4	100	10000
MAP4K2	MAP4K2	92	10000
MAP4K3	MAP4K3	90	10000
MAP4K4	MAP4K4	72	10000
MAP4K5	MAP4K5	80	10000
MAPKAPK2	MAPKAPK2	100	10000
MAPKAPK5	MAPKAPK5	100	10000
MARK1	MARK1	100	10000
MARK2	MARK2	79	10000
MARK3	MARK3	100	10000
MARK4	MARK4	99	10000
MAST1	MAST1	40	10000
MEK1	MAP2K1	100	10000
MEK2	MAP2K2	100	10000
MEK3	MAP2K3	87	10000
MEK4	MAP2K4	98	10000
MEK5	MAP2K5	2.2	10000
MEK6	MAP2K6	100	10000
MELK	MELK	98	10000
MERTK	MERTK	100	10000
MET	MET	96	10000
MET(M1250T)	MET	90	10000
MET(Y1235D)	MET	60	10000
MINK	MINK1	88	10000
MKK7	MAP2K7	86	10000
MKNK1	MKNK1	100	10000
MKNK2	MKNK2	67	10000
MLCK	MYLK3	100	10000
MLK1	MAP3K9	99	10000
MLK2	MAP3K10	70	10000
MLK3	MAP3K11	90	10000
MRCKA	CDC42BPA	94	10000
MRCKB	CDC42BPB	89	10000
MST1	STK4	87	10000
MST1R	MST1R	67	10000
MST2	STK3	54	10000
MST3	STK24	95	10000

MST4	MST4	90	10000
MTOR	MTOR	16	10000
MUSK	MUSK	87	10000
MYLK	MYLK	85	10000
MYLK2	MYLK2	100	10000
MYLK4	MYLK4	98	10000
MYO3A	MYO3A	97	10000
MYO3B	MYO3B	89	10000
NDR1	STK38	86	10000
NDR2	STK38L	91	10000
NEK1	NEK1	100	10000
NEK10	NEK10	89	10000
NEK11	NEK11	85	10000
NEK2	NEK2	86	10000
NEK3	NEK3	60	10000
NEK4	NEK4	76	10000
NEK5	NEK5	100	10000
NEK6	NEK6	93	10000
NEK7	NEK7	76	10000
NEK9	NEK9	78	10000
NIK	MAP3K14	100	10000
NIM1	MGC42105	89	10000
NLK	NLK	100	10000
OSR1	OXSR1	100	10000
p38-alpha	MAPK14	88	10000
p38-beta	MAPK11	96	10000
p38-delta	MAPK13	81	10000
p38-gamma	MAPK12	75	10000
PAK1	PAK1	100	10000
PAK2	PAK2	100	10000
PAK3	PAK3	66	10000
PAK4	PAK4	99	10000
PAK6	PAK6	88	10000
PAK7	PAK7	74	10000
PCTK1	CDK16	100	10000
PCTK2	CDK17	100	10000
PCTK3	CDK18	78	10000
PDGFRA	PDGFRA	97	10000
PDGFRB	PDGFRB	76	10000
PDPK1	PDPK1	67	10000
PFCDPK1(P.falciparum)	CDPK1	88	10000

PFPK5(P.falciparum)	MAL13P1.279	100	10000
PFTAIRE2	CDK15	90	10000
PFTK1	CDK14	95	10000
PHKG1	PHKG1	100	10000
PHKG2	PHKG2	92	10000
PIK3C2B	PIK3C2B	5	10000
PIK3C2G	PIK3C2G	23	10000
PIK3CA	PIK3CA	0	10000
PIK3CA(C420R)	PIK3CA	0.85	10000
PIK3CA(E542K)	PIK3CA	0.6	10000
PIK3CA(E545A)	PIK3CA	0.65	10000
PIK3CA(E545K)	PIK3CA	0.65	10000
PIK3CA(H1047L)	PIK3CA	0.3	10000
PIK3CA(H1047Y)	PIK3CA	0	10000
PIK3CA(I800L)	PIK3CA	1.6	10000
PIK3CA(M1043I)	PIK3CA	1.4	10000
PIK3CA(Q546K)	PIK3CA	0.6	10000
PIK3CB	PIK3CB	5.9	10000
PIK3CD	PIK3CD	7.4	10000
PIK3CG	PIK3CG	43	10000
PIK4CB	PI4KB	56	10000
PIKFYVE	PIKFYVE	46	10000
PIM1	PIM1	100	10000
PIM2	PIM2	74	10000
PIM3	PIM3	100	10000
PIP5K1A	PIP5K1A	100	10000
PIP5K1C	PIP5K1C	100	10000
PIP5K2B	PIP4K2B	100	10000
PIP5K2C	PIP4K2C	90	10000
PKAC-alpha	PRKACA	59	10000
PKAC-beta	PRKACB	98	10000
PKMYT1	PKMYT1	92	10000
PKN1	PKN1	79	10000
PKN2	PKN2	85	10000
PKNB(M.tuberculosis)	pknB	79	10000
PLK1	PLK1	100	10000
PLK2	PLK2	89	10000
PLK3	PLK3	84	10000
PLK4	PLK4	72	10000
PRKCD	PRKCD	93	10000
PRKCE	PRKCE	100	10000

PRKCH	PRKCH	91	10000
PRKCI	PRKCI	79	10000
PRKCQ	PRKCQ	85	10000
PRKD1	PRKD1	100	10000
PRKD2	PRKD2	100	10000
PRKD3	PRKD3	94	10000
PRKG1	PRKG1	98	10000
PRKG2	PRKG2	96	10000
PRKR	EIF2AK2	100	10000
PRKX	PRKX	88	10000
PRP4	PRPF4B	72	10000
PYK2	PTK2B	85	10000
QSK	KIAA0999	80	10000
RAF1	RAF1	94	10000
RET	RET	99	10000
RET(M918T)	RET	100	10000
RET(V804L)	RET	100	10000
RET(V804M)	RET	93	10000
RIOK1	RIOK1	79	10000
RIOK2	RIOK2	90	10000
RIOK3	RIOK3	89	10000
RIPK1	RIPK1	100	10000
RIPK2	RIPK2	84	10000
RIPK4	RIPK4	70	10000
RIPK5	DSTYK	78	10000
ROCK1	ROCK1	95	10000
ROCK2	ROCK2	85	10000
ROS1	ROS1	93	10000
RPS6KA4(Kin.Dom.1-N-terminal)	RPS6KA4	98	10000
RPS6KA4(Kin.Dom.2-C-terminal)	RPS6KA4	95	10000
RPS6KA5(Kin.Dom.1-N-terminal)	RPS6KA5	85	10000
RPS6KA5(Kin.Dom.2-C-terminal)	RPS6KA5	100	10000
RSK1(Kin.Dom.1-N-terminal)	RPS6KA1	88	10000
RSK1(Kin.Dom.2-C-terminal)	RPS6KA1	93	10000
RSK2(Kin.Dom.1-N-terminal)	RPS6KA3	78	10000
RSK2(Kin.Dom.2-C-terminal)	RPS6KA3	86	10000
RSK3(Kin.Dom.1-N-terminal)	RPS6KA2	85	10000
RSK3(Kin.Dom.2-C-terminal)	RPS6KA2	92	10000
RSK4(Kin.Dom.1-N-terminal)	RPS6KA6	96	10000
RSK4(Kin.Dom.2-C-terminal)	RPS6KA6	93	10000
S6K1	RPS6KB1	85	10000

SBK1	SBK1	100	10000
SGK	SGK1	98	10000
SgK110	SgK110	100	10000
SGK2	SGK2	89	10000
SGK3	SGK3	70	10000
SIK	SIK1	96	10000
SIK2	SIK2	94	10000
SLK	SLK	92	10000
SNARK	NUAK2	91	10000
SNRK	SNRK	95	10000
SRC	SRC	59	10000
SRMS	SRMS	71	10000
SRPK1	SRPK1	92	10000
SRPK2	SRPK2	100	10000
SRPK3	SRPK3	97	10000
STK16	STK16	84	10000
STK33	STK33	95	10000
STK35	STK35	93	10000
STK36	STK36	98	10000
STK39	STK39	91	10000
SYK	SYK	88	10000
TAK1	MAP3K7	73	10000
TAOK1	TAOK1	80	10000
TAOK2	TAOK2	100	10000
TAOK3	TAOK3	95	10000
TBK1	TBK1	75	10000
TEC	TEC	97	10000
TESK1	TESK1	90	10000
TGFBR1	TGFBR1	97	10000
TGFBR2	TGFBR2	80	10000
TIE1	TIE1	82	10000
TIE2	TEK	100	10000
TLK1	TLK1	90	10000
TLK2	TLK2	100	10000
TNIK	TNIK	100	10000
TNK1	TNK1	63	10000
TNK2	TNK2	100	10000
TNNI3K	TNNI3K	75	10000
TRKA	NTRK1	45	10000
TRKB	NTRK2	87	10000
TRKC	NTRK3	100	10000

TRPM6	TRPM6	77	10000
TSSK1B	TSSK1B	98	10000
TSSK3	TSSK3	100	10000
TTK	TTK	75	10000
TXK	TXK	89	10000
TYK2(JH1domain-catalytic)	TYK2	91	10000
TYK2(JH2domain-pseudokinase)	TYK2	99	10000
TYRO3	TYRO3	100	10000
ULK1	ULK1	100	10000
ULK2	ULK2	95	10000
ULK3	ULK3	83	10000
VEGFR2	KDR	93	10000
VPS34	PIK3C3	12	10000
VRK2	VRK2	94	10000
WEE1	WEE1	80	10000
WEE2	WEE2	81	10000
WNK1	WNK1	100	10000
WNK2	WNK2	99	10000
WNK3	WNK3	100	10000
WNK4	WNK4	100	10000
YANK1	STK32A	99	10000
YANK2	STK32B	95	10000
YANK3	STK32C	95	10000
YES	YES1	100	10000
YSK1	STK25	100	10000
YSK4	MAP3K19	80	10000
ZAK	ZAK	93	10000
ZAP70	ZAP70	100	10000